Transcriptomic analyses of MYCN-regulated genes in anaplastic Wilms' tumour cell lines reveals oncogenic pathways and potential therapeutic vulnerabilities

Marianna Szemes[1*], Zsombor Melegh[2], Jacob Bellamy[1], Ji Hyun Park[1], Biyao Chen[1], Alexander Greenhough[1,3], Daniel Catchpoole[4] and Karim Malik[1*]

[1]Cancer Epigenetics Laboratory, School of Cellular and Molecular Medicine, University of Bristol, Bristol, UK.

[2]Department of Cellular Pathology, Southmead Hospital, Bristol, UK.

[3]Applied Sciences, University of the West of England. Bristol, UK.

[4]The Kids Research Institute, The Children's Hospital at Westmead, Westmead, New South Wales 2145, Australia.

*** Correspondence:** K.T.A.Malik@bristol.ac.uk; M.Szemes@bristol.ac.uk

Running title: Transcriptomic analysis of MYCN-regulated genes in Wilms' tumour

Keywords: Wilms' tumour, MYCN, REST, PRMT, TOMM20, RNA-seq.

Abbreviations:

ADMA	asymmetric di-methyl arginine
CM	condensing mesenchyme
DEG	differentially expressed genes
ECL	enhanced chemiluminescence
FACS	fluorescence activated cell sorting
FDR	false discovery rate
FHWT	favourable histology Wilms' tumour
FK	fetal kidney

GO	Gene ontology
GSEA	Geneset Enrichment Analysis
HRP	horseradish peroxidase
IHC	immunohistochemistry
MNA	MYCN-amplified
NB	neuroblastoma
NES	normalised enrichment score
PTA	pre-tubular aggregates
R-Me	arginine methylation
SDMA	symmetric di-methyl arginine
TIM	translocase of the inner membrane
TMA	tissue microarray
TOM	translocase of the outer membrane
UB	ureteric bud
WT	Wilms' tumour

Abstract

The *MYCN* proto-oncogene is deregulated in many cancers, most notably in neuroblastoma where *MYCN* gene amplification identifies a clinical subset with very poor prognosis. Gene expression and DNA analyses have also demonstrated over-expression of *MYCN* mRNA, as well as focal amplifications, copy number gains and presumptive change of function mutations of *MYCN* in Wilms' tumours with poorer outcome, including tumours with diffuse anaplasia. Surpisingly, however, the expression and functions of the MYCN protein in Wilms' tumours still remain obscure.

In this study, we assessed MYCN protein expression in primary Wilms' tumours using immunohistochemistry of tissue microarrays. We found MYCN protein to be expressed in tumour blastemal cells, and absent in stromal and epithelial components. For functional studies, we used two anaplastic Wilms' tumour cell-lines, WiT49 and 17.94, to study the biological and transcriptomic effects of MYCN depletion. We found that MYCN knockdown consistently led to growth suppression but not cell death. RNA sequencing identified 561 MYCN-regulated genes shared by WiT49 and 17.94 cell-lines. As expected, numerous cellular processes were downstream of MYCN. MYCN positively regulated the miRNA regulator and known Wilms' tumour oncogene *LIN28B*, the genes encoding methylosome proteins PRMT1, PRMT5 and WDR77, and the mitochondrial translocase genes *TOMM20* and *TIMM50*. MYCN repressed genes included the developmental signalling receptor *ROBO1* and the stromal marker *COL1A1*. Importantly, we found that MYCN also repressed the presumptive Wilms' tumour suppressor gene *REST*, with MYCN knockdown resulting in increased REST protein and concomitant repression of REST target genes. Together, our study

identifies regulatory axes that interact with MYCN, providing novel pathways for potential targeted therapeutics for poor prognosis Wilms' tumour.

1. Introduction

Wilms' tumour (WT) is the most common paediatric renal malignancy. WT can broadly be categorized as favourable histology (FHWT) or anaplastic. Whilst survival of FHWT patients after neoadjuvant therapy has improved overall survival, patients often relapse and experience extensive side-effects as a result of current therapies, with survivors remaining at elevated risk for death long after their diagnosis. Stage III-IV tumours, including anaplastic WT can have markedly worse prognosis, with a 4-year survival rate as low as ~50%. Thus there remains a critical requirement for more personalised, targeted therapies to prevent severe illness and death from WT (1,2).

The earliest genetic analyses of WT showed loss-of-function mutations in *WT1* (3,4), missense *TP53* mutations (5) and gain-of-function *CTNNB1* mutations resulting in activation of Wnt signalling (6). These mutations segregate with WT subtypes, for example *WT1* and *CTNNB1* mutations in stromal-predominant WT, and *TP53* in anaplastic WTs (5,7,8). More recent genome sequencing studies have found further mutations, including *MYCN*, *REST*, *SIX1/2*, *DROSHA* and *DICER* (7-9), reported in approximately half of all WTs. Inactivating mutations of *REST* were also independently reported, implicating it as a WT tumour suppressor gene in familial and non-familial WT (10).

Together with previous studies demonstrating *MYCN* gain and *FBXW7* loss associated with diffuse anaplasia and poorer outcome even in the absence of anaplasia, and focal amplifications of *MYCN* in anaplastic WTs (11,12), these whole-genome sequencing analyses suggest an oncogenic role for MYCN in WT. This is further supported by the fact that several groups documented *MYCN* mRNA over-expression in WTs, and its association with poor prognosis (13-15). Together

this strongly implicates *MYCN* deregulation in Wilms' tumorigenesis. However, despite MYCN being known to be important in proliferation of mesenchymal progenitor cells during nephrogenesis (16) and an established oncogenic transcription factor of developmental cancers such as medulloblastoma and neuroblastoma (NB) (17), virtually nothing is known about the biological activities of MYCN in WT, including protein expression patterns, downstream transcriptional targets, and possible pathways regulated.

In this study, we report the first analysis of MYCN protein in primary WTs. Furthermore, our functional analyses demonstrate that MYCN regulates proliferation of anaplastic WT cell-lines. RNA sequencing of these cell-lines after MYCN depletion identifies novel growth control pathways regulated by MYCN, including intersection with the function of the putative WT tumour suppressor gene, *REST* (RE1-Silencing Transcription factor).

2. Materials and Methods

2.1. Wilms' tumour cell-lines, culture conditions and siRNA treatments

Wit49 (18) and 17.94 (19) anaplastic WT cell-lines were kind gifts from Prof. Herman Yeger and Dr. Keith Brown, respectively. The identity of both cell-lines was confirmed by short tandem repeat (STR) analysis. Wit49 cells were cultured at 37°C under 5% CO_2, in Dulbecco's modified Eagle's medium supplemented with 15% fetal calf serum, 2 mmol/L L-glutamine, 0.1 mg/mL penicillin/streptomycin, 0.6%(v/v) β-mercaptoethanol and 1x insulin–transferrin–selenium, all purchased from Sigma. 17.94 cells were grown in Dulbecco's modified Eagle's medium supplemented with 10% fetal calf serum, L-glutamine and penicillin and streptomycin. Absence of Mycoplasma infection was confirmed by Mycoalert Mycoplasma Detection Kit (Lonza). Knock-down experiments were performed by using RNAiMAX reagent (Invitrogen) with 20 nM siRNA, according to manufacturer's instructions. Oligonucleotide sequences are shown in Supplementary Table 1.

2.2. Cell cycle analysis and cell counting

Propidium-iodide labelling and fluorescence activated cell sorting (FACS) analysis was used to detect cell cycle phases. Floating and adherent cells were collected, washed with PBS, fixed with ice cold 70% (v/v) ethanol and treated with RNase A (Qiagen). After adding 50 µg/mL Propidium Iodide (Sigma), the samples were incubated at 37ºC for 15 minutes, and analysed on Fluorescence Activated Cell Sorter LSRFortessaTM X-20 (BD Biosciences). About 15,000 events were collected for each replicate and data was analyzed by using FlowJo software. Cell counting was performed by using Countess automated cell counter (Invitrogen) and trypan blue staining.

2.3. Immunohistochemistry

Tissue microarrays, containing 33 pre-chemotherapy, Wilms' tumor samples and fetal and adult kidney sections were stained by using a MYCN antibody (Proteintech, 10159-2-AP, Lot no: 18121). Immunohistochemistry staining was scored as positive or negative by a pathologist blinded to the specimens. All human tissues were acquired in compliance with the NSW Human Tissue and Anatomy Legislation Amendment Act 2003 (Australia). Ethics clearances 09/CHW/159 and LNR/14/SCHN/392 were approved by the Sydney Children's Hospital Network Human Research Ethics Committee to construct TMAs and use clinical data, which was deidentified. Immunohistochemistry was performed with a Leica Microsystem Bond III automated machine by using the Bond Polymer Refine Detection Kit (Ref DS9800) followed by Bond Dab Enhancer (AR9432). The slides were dewaxed with Bond Dewax Solution (AR9222) and heat mediated antigen retrieval was performed using Bond Epitope Retrieval Solution for 20 minutes.

2.4. Protein Extraction and Western Blot

Cells were lysed in Radioimmunoprecipitation assay (RIPA) buffer and protein concentration was determined by using Micro BCA TM protein assay kit (Thermo Fisher). Protein extracts were loaded onto SDS poly-acrylamide gels and run in 1x Tris-glycine SDS buffer. After transfer onto PVDF membrane (Millipore) by a wet protocol (Bio-Rad), the membrane was blocked in 5% (w/v) skimmed milk, incubated with primary antibody solution at 4 ºC overnight, and HRP labelled secondary antibody solution the next day. Proteins were visualised by using ECL reagents (Lumiglo, KPL) and X-ray films. The antibodies used are listed in Supplementary Table 2. Western blot image data were quantified by using ImageJ

156 software (http://imagej.nih.gov/ij/). Target protein band density was normalized to
157 the respective loading control and to the normalized intensity of the control sample.

158 ***2.5. RNA extraction, reverse transcription and qPCR***

159 RNA was extracted by using the miRNeasy kit (QIAGEN), according to
160 manufacturer's instructions. RNAs were treated with on column DNase digestion
161 using RNase-free DNase (Qiagen). RNA was transcribed with Superscript IV
162 (Invitrogen) using a mixture of oligodT and random hexamer primers. Quantitative
163 PCR was performed by using QuantiNova kit (Qiagen) on Mx3500P (Stratagene).
164 The house-keeping gene TBP was used as a normalizing control. Relative gene
165 expression was calculated using the ΔΔCt method – log2 fold changes between
166 MYCN-depleted and control samples were calculated after normalization to TBP.
167 Statistical significance of log2-transformed fold changes in gene expression was
168 evaluated by using two-tailed, Student's T-tests. The oligonucleotide primers used
169 in this study are shown in Supplementary Table 1.

170 ***2.6. RNA-seq and bioinformatic analysis***

171 Wit49 and 17.94 cells were treated with MYCN-targeting and control siRNAs
172 for 48 hours, and were subsequently harvested in Qiazol (Qiagen). RNA was
173 extracted by using the miRNeasy Kit (Qiagen). RNA concentration and quality were
174 checked by using a Nanodrop spectrophotometer and Bioanalyzer (Agilent).
175 Libraries were prepared from 200 ng RNA and were sequenced by using the
176 paired-end option with 100 bp reads on BGIseq-500 (BGI Genomics). The reads
177 were aligned to the human genome (hg38) by using STAR and the alignment files
178 (BAM) files were further analysed in SeqMonk v1.47.
179 (https://www.bioinformatics.babraham.ac.uk/projects/seqmonk/). Gene expression
180 was quantified by using the Seqmonk RNA-seq analysis pipeline and differentially

expressed genes (DEG) were identified by DESEQ2 ($p<0.05$), and a minimum shrunk fold difference threshold, a conservative corrected value of fold change taking confidence into account, of 1.2 was applied. RNA sequencing data is available from the European Nucleotide Archive (ENA) under the accession number ERP125499. Gene Signature Enrichment Analyses (GSEAs) were performed on preranked lists of log2-transformed, shrunk fold difference gene expression values (Broad Institute). Gene expression analysis of published Wilms' tumour data sets and K means clustering were performed by using the R2 Genomics Analysis and Visualization Platform (http://r2.amc.nl).

2.7 Statistical analysis

Statistical analysis of quantitative PCR data was performed on log2-transformed fold change values, by using two-tailed Student's T-tests. Gene Set Enrichment Analysis of RNA-seq data was evaluated based on Normalised Enrichment Score (NES) and False Discovery Rate (FDR), which was calculated based on permutation of genes with a rank score of log2 fold change expression over control. Differentially expressed genes (DEGs) in MYCN-depleted Wilms' tumour cells, detected by using RNA-seq, were assessed using the statistical model implemented in DESEQ2. Significance of correlation between clusters of TARGET WT data and clinical correlates was assessed by using Chi-square test. Differential expression of genes and metagenes, which represent gene signatures, among groups of WT and fetal kidney tissue, was evaluated by using ANOVA.

3. Results & Discussion

3.1 MYCN protein is overexpressed in the blastemal component of Wilms' tumour and promotes proliferation in Wilms' tumour cells.

Over-expression of *MYCN* mRNA has been reported in poor prognosis Wilms' tumour (13-15,20) but the prevalence and pattern of MYCN protein expression in Wilms' tumours has, to our knowledge, never been published. Therefore, we performed MYCN immunohistochemistry (IHC) on tissue microarrays (TMAs), containing 33 pre-chemotherapy WT sections (Figure 1). As a normal control, we used a section of a fetal kidney, derived from a 13-week old fetus, as well as an adult, healthy kidney. MYCN was detected in 14 tumours, exclusively in the blastemal component. It was localised mostly to the nucleus, but we also detected cytoplasmic staining, with three tumours displaying cytoplasmic staining only. In contrast, in normal fetal kidney, MYCN was detected solely in the distal tubules, but not in the blastema, while MYCN protein was completely absent from the adult kidney (Supplementary figure 1). Although the number of tumours precluded statistical analysis, our data demonstrates for the first time that MYCN protein is expressed in the blastemal cells of Wilms' tumours.

To characterize the effect of MYCN on growth of Wilms' tumour cells, we knocked it down in two anaplastic WT cell-lines, Wit49 and 17.94 (Figure 2). After 120 hours of MYCN depletion by two independent MYCN-targeting siRNAs, there was a substantial and significant reduction in live cell counts ($p < 0.01$). The number of dead cells did not increase, suggesting that the decrease in live cells was due to growth inhibition rather than increased cell death. To investigate the effect of MYCN depletion on the cell cycle, we performed a cell cycle analysis on Wit49 (Supplementary figure 2). MYCN knock-down by either siRNA led to a significant

reduction of cells in S phase, while the proportion of cells in G2/M increased significantly ($p < 0.01$), indicative of a G2/M arrest. There was no increase of cells in the sub-G1 phase, in agreement with our previous observation of no increase in dead cell counts. These studies suggest that MYCN primarily exerts control over WT proliferative pathways as opposed to apoptosis and cell survival.

3.2 MYCN-regulated gene signatures in Wilms' tumour reveal downstream growth-regulatory pathways

To identify MYCN regulated genes in Wilms' tumour, we performed RNA-seq of both anaplastic WT cell-lines following MYCN knockdown (Supplementary figure 3A). MYCN regulated genes were defined as differentially expressed genes (DEGs) that had a significant ($p < 0.05$) and substantial change (minimum 'shrunk' fold change, a corrected value based on confidence, of 1.2) in their expression levels, as assessed by using DESEQ2. We found 1060 upregulated genes in Wit49 and 396 in 17.94, with a highly significant overlap of 212 genes between the 2 cell-lines ($p < 10^{-10}$) (Figure 3A). There were 349 downregulated genes shared by the two cell-lines, with 1086 and 699 identified in Wit49 and 17.94, respectively ($p < 10^{-10}$). The shared 561 MYCN-regulated genes in WT are shown in Supplementary table 3. and Figure 3B. Known MYCN target genes, and genes related to WT or kidney development are highlighted on the heatmaps. A panel of the DEGs identified by RNA-seq after MYCN knockdown were validated in both cell-lines by qPCR. We confirmed downregulation of *LIN28B*, a MYCN target gene in neuroblastoma (21), both at the RNA (Figure 3C) and protein level (Supplementary figure 3B). LIN28B is an established regulator of nephrogenesis, promoting expansion of the progenitor pool, and a direct oncogenic driver in WT (22,23). LIN28B suppresses *let-7* miRNAs, but can also influence gene expression via other mechanisms, including

253 regulation of translation (24). Therefore MYCN is likely to exert control at the post-
254 transcriptional as well as the transcriptomic level.

255 Amongst the novel genes, one of the biggest expression changes was the
256 *ROBO1* gene, which increased over 4-fold after MYCN knockdown in both WT cell-
257 lines (Figure 3C). *ROBO1* encodes the transmembrane Roundabout Guidance
258 Receptor 1 involved in SLIT/ROBO signalling, a key developmental pathway (25).
259 *Robo1* is a tumour suppressor gene in other cellular systems, with *Robo1* knockout
260 mice predisposing to lung adenocarcinomas and lymphomas (26). Other studies
261 have indicated that Slit/Robo signalling is required for normal kidney development
262 (27), and *Robo1* expression increases in the pretubular aggregates compared to
263 the metanephric mesenchyme, implying a role for Robo1 in early renal
264 differentiation (28). We also note that *SLIT2* is frequently epigenetically silenced in
265 WTs (29), further supporting a tumour suppressive role for SLIT/ROBO signalling in
266 WT.

267 Gene set enrichment analysis indicated that MYCN repressed kidney
268 differentiation and developmental genes (Supplementary figure 3C). To study how
269 MYCN influences cell differentiation during nephrogenesis, we queried gene
270 signatures characteristic of different cell populations in the fetal kidney, determined
271 by Menon et al. by using single cell RNA-seq (30). We found that MYCN activated
272 genes were overexpressed in proliferating cells, while gene signatures of both
273 podocytes and stromal cells were repressed by MYCN, consistent with a role for
274 MYCN in promoting growth and repressing differentiation (Supplementary Figure
275 3D). *COL1A1,* a marker gene for stromal cells, was upregulated more than two-fold
276 in our RNA-seq data after MYCN depletion. Moreover, COL1A1 protein is

documented to be significantly downregulated in anaplastic WT compared to favorable histology WT (31).

MYCN targets have been extensively studied in NB and several target lists were described. We compared our WT-specific MYCN targets to some identified by transcriptomic and chromatin immunoprecipitation analyses in NB, specifically (i) the MYCN157 signature, derived from IMR32 cell-line DEGs following MYCN knockdown, subsequently filtered by correlation with MYCN mRNA expression in primary NBs (32), (ii) DEGs from a MYCN-overexpressing isogenic model (33) and (iii) genes bound by MYCN and correlated with MYCN in the SEQC NB expression dataset (GSE49712) (34) (Figure 3D). We found surprisingly little overlap of our top DEGs with these NB-specific MYCN targets, emphasizing the importance of cellular context. To characterize the function of the newly identified MYCN regulated genes, we performed a Gene Ontology (GO) enrichment analysis (Supplementary table 4.). The most highly enriched component was the 'RNA nuclear export complex' (GO:0042565), including *XPO5* and *RAN*, responsible for the transport of pre-miRNAs from the nucleus, suggesting that MYCN may substantially alter the miRNA profile in the cytoplasm. Mutations in *DICER* and *DROSHA*, key enzymes in microRNA biogenesis, were previously shown to be involved in WT pathogenesis (8). The WT-specific MYCN regulated genes were also enriched in GO categories related to mitochondrial, ribosomal, spliceosomal and methylosome complexes and telomere maintenance, emphasising the control of several major cellular processes by MYCN.

To obtain an extended global overview of the transcriptional control of MYCN in WT, we performed Gene Set Enrichment Analyses (GSEA) with the DEGs from Wit49 and 17.94 cell-lines. GSEA revealed that MYCN knockdown led to activation

of genes downregulated in WT relative to fetal kidney (Figure 3E) (35), and repression of genes elevated in WT relative to fetal kidney (Supplementary Figure 4A). Thus MYCN knockdown reverses, at least in part, the WT-specific signature.

MYCN activated genes in the MYCN157 signature were significantly downregulated, showing regulation of the NB-specific target genes in WT cells, despite the minimal overlap of our top DEGs (with the biggest or most significant changes) with top MYCN targets in NB. Similarly, several MYC target gene sets were downregulated in both cell-lines, indicating that MYCN drives canonical MYC target genes in WT (Supplementary figure 4B), like the curated MYC gene set in Hallmark (36). Further, genes encoding mitochondrial proteins that were recently shown to be regulated by MYCN (37) were also down-regulated, emphasizing the role of MYCN in activating mitochondrial function genes in WT. Genes encoding for proteins with roles in 'RNA export from nucleus' were down-regulated, which may affect pre-miRNA transport and the miRNA pool in the cytoplasm, while those participating in 'Unfolded protein response' were up, suggestive of endoplasmic reticulum stress in the MYCN depleted cells (Supplementary figure 4C).

Gene signatures related to ribosomal biogenesis, splicing, and mitochondria were all found to be down-regulated following MYCN knockdown, reinforcing the results of GO analysis with shared WT-specific MYCN-regulated genes (Figure 3E). In fact, all the Gene Ontology signatures related to to ribosomal function, RNA processing/splicing, and mitochondria were found to be profoundly downregulated in both MYCN depleted cell lines, suggesting a strong activation of these gene expression programmes by MYCN in WT (Figure 3F).

Ribosomal biogenesis was reported to be upregulated in *MYCN*-amplified neuroblastoma too, and inhibitors of RNA polymerase I (which transcribes

ribosomal RNA genes) suppressed MYCN expression and promoted apoptosis of MNA NB cells, both *in vitro* and *in vivo* (38). Deregulation of splicing (39) and metabolic reprogramming by MYCN (40) were also observed in neuroblastoma, consistent with our transcriptomic analysis in WT.

To investigate the expression of *MYCN* and its target genes in a large set of primary Wilms' tumour tissue, we analysed the publicly available WT RNA-seq data set, TARGET-WT (SRP012006), containing expression data for 124 high-risk tumours. We found a strong and highly significant, positive correlation between the expression of *MYCN* and its activated target genes in WT ($R = 0.43$, $p = 5.6 \times 10^{-7}$), suggesting a regulatory link *in vivo* (Figure 4A). The correlation between *MYCN* and the newly identified repressed genes in the tumours is less pronounced and does not reach significance ($R = -0.15$, $p = 0.087$), suggesting that other regulators might also be involved in repression. For example, *LIN28B* was reported to be activated via chromosomal translocation and amplification in WT, independent of MYCN (41) and *REST* can be inactivated via mutations. To identify the tumours with a MYCN-regulated signature and study their clinical correlates, we clustered the WT transcriptomic data set according to the expression of the shared 561 MYCN target genes (Figure 4B). Two clusters were identified: a larger group (cluster 1) with a mostly uniform expression of target genes and a smaller group of 14 tumours (cluster 2), displaying up-regulated and down-regulated subsets of our MYCN target genes. The tumours in cluster 2 were generally higher stages, with a significant difference in distribution (Chi squared test $p = 0.015$, Figure 4C). Cluster 1 contained all the stage 1 tumours, and the proportion of stage 2 ones was higher as well (43% vs. 14%). In contrast, there was a higher proportion of stage 3 and 3B tumours in cluster 2: 71% vs. 28% and 7% vs. 3%, respectively. Patients with

352 tumours in the MYCN-regulated group (cluster 2) had lower survival (42.9% vs.
353 61.8%), although this trend did not reach significance probably because of the
354 relatively low number of patient samples in cluster 2 (Figure 4D).
355 To evaluate the expression of functional gene sets in primary Wilms'
356 tumours, we assessed the overall expression of GO gene categories highlighted by
357 our RNA-seq analysis, represented as metagenes, in the newly defined clusters in
358 TARGET-WT (Figure 4E). Ribosomal genes had a significantly and substantially
359 higher expression in cluster 2 than cluster 1 ($p = 3.2 \times 10^{-15}$). Genes coding for
360 mitochondrial protein complexes ($p = 3.8 \times 10^{-13}$) and methylosome components (p
361 $= 4.7 \times 10^{-8}$) were similarly significantly upregulated in cluster 2, reinforcing our data
362 in WT cell-lines. Together these analyses show that the DEGs we identified in
363 Wit49 and 17.94 cell-lines correlate with MYCN in primary WTs, and that pathways
364 identified by our *in vitro* analyses are aberrant in a subset of higher stage WTs.

365 ***3.3 MYCN upregulates key mitochondrial transporter gene TOMM20,***
366 ***overexpressed in blastemal and relapsed WT***

367 Gene set enrichment analysis revealed a profound downregulation of genes
368 encoding for mitochondrial complexes upon MYCN depletion, in both anaplastic WT
369 cell-lines (Figure 5A). The most downregulated genes included *TOMM20* (Figure
370 5B), encoding a member of the translocase of the outer membrane (TOM) complex,
371 responsible for the import of newly synthesized mitochondrial proteins from the
372 cytosol. The TOM complex works in close co-operation with the translocase of the
373 inner membrane (TIM) complex (42), a key member of which, *TIMM50*, was also
374 downregulated with MYCN depletion. We confirmed the downregulation of these
375 mitochondrial protein genes together with *PDK1* by qPCR (Figure 5C); PDK1
376 (Pyruvate Dehydrogenase Kinase 1) is a gatekeeper of the Warburg effect and

frequently overexpressed in cancer (43). Downregulation of TOMM20 was also confirmed at the protein level in both anaplastic WT lines (Figure 5D). In the TARGET-WT RNA-seq dataset, we observed a significant, positive correlation between the expression of *MYCN* and *TOMM20*, consistent with our findings (Figure 5E). *TOMM20* was inferred to be a MYCN target gene in neuroblastoma due to MYCN binding to its promoter and its mRNA positively correlating with MYCN (34). However, our data at both protein and RNA levels demonstrate for the first time that TOMM20 is directly regulated by MYCN. In two other, publicly available transcriptomic data sets by Perlman et al. (44,45), *TOMM20* was found to be significantly overexpressed in relapsed WT vs. non-relapsed (Figure 5F) and in blastemal tumours relative to other tumours (Figure 5G). *TOMM20* over-expression is associated with poor prognosis in other cancers such as colorectal cancer and chondrosarcoma (46,47), and TOMM20 knockdown in colorectal cancer cells led to increased mitochondrial damage, significantly reduced ATP production and apoptosis *in vitro*, and reduced growth of tumour xenografts *in vivo*. Whilst metabolic defects in WT are not extensively studied, it has been demonstrated that stromal tumours have markedly reduced mitochondrial mass and function compared to blastemal tumours, and that oxidative phosphorylation is considerably lower in WT than normal kidney (48). Taken together with our data, this invokes the possibility that MYCN-regulated over-expression of TOMM20 may alter mitochondrial protein import by the TOM complex and facilitate the glycolytic switch (Warburg effect) in poor prognosis WT. In this regard, it is interesting to note that TOMM20 over-expression has been demonstrated to retard mitochondrial protein import, presumably by disruption of the normal stoichiometry of subunits of the import receptor complex (49).

3.4 MYCN upregulates methylosome components in WT and influences post-translational regulation via promoting arginine methylation

The methylosome was one of the most enriched GO categories in our transcriptomic analysis of MYCN depletion in WT cells, with six out of the 12 members significantly downregulated in both cell-lines. A heatmap of the methylosome genes shows that the other six members were also downregulated, albeit to a lesser extent (Figure 6A). Expression changes of *WDR77*, encoding for MEP50, and *PRMT1* were validated by using qPCR (Figure 6B). Analysis of RNA-seq data indicated that *PRMT5* was also downregulated in both cell-lines, although to a lesser extent.

Downregulation was confirmed at the protein level for three key methylosome components: PRMT1, catalysing asymmetrical arginine di-methylation (ADMA), PRMT5 and WDR77/MEP50, acting in a complex to effect symmetrical arginine di-methylation (SDMA) modification (Figure 6C). We hypothesized that such profound downregulation of the methylosome components may influence global arginine di-methylation levels, which we tested by using antibodies against ADMA and SDMA modifications. We found that ADMA levels were reduced with MYCN depletion in both cell-lines by using two different siRNAs. SDMA modification was also reduced in the 15 - 20 kDa size range, suggesting reduction of SDMA marks of snRNP proteins, which participate in RNA splicing.

Our analyses further established that *PRMT1* and *WDR77* were significantly overexpressed in WT as compared to fetal kidney in the transcriptomic data set published by Li et al. (35) (Figure 6D), supporting a role for arginine methyltransferases in WT pathogenesis. Both *PRMT1* and *WDR77* are MYCN targets within the MYCN157 geneset for poor prognosis NB (32) and MYCN also

binds the *PRMT5* promoter (50). PRMTs are often over-expressed in cancer (51), and we have previously shown that PRMT5 is a survival factor for MYCN-amplified NB, with PRMT5 interacting with and methylating MYCN protein (52). We have also shown that neuroblastoma cells are sensitive to PRMT1 inhibition (53). Small molecule inhibitors of PRMTs have been developed recently and demonstrated to have efficacy *in vitro* and *in vivo* against cancers such as mantle cell lymphoma (54,55) and are currently in clinical trials for solid tumours and various forms of leukemia (56). Our transcriptomic and protein level analyses suggest that a PRMT-MYCN axis may also be involved in WT, and that selective inhibition of PRMTs may represent a novel targeted therapy for poor prognosis WT.

3.5 MYCN represses WT predisposition gene REST, leading to activation of its target genes

Exome sequencing of familial and non-familial Wilms' tumors recently revealed loss of function mutations in the *REST* gene (encoding RE1 Silencing Transcription Factor) (10). REST is a Krüppel-type zinc-finger transcription factor which acts as a repressor of gene transcription via numerous interactions with chromatin-modifiers, and deregulation of REST is implicated in the pathogenesis of several diseases, including cancer (57). Intriguingly, our RNA-seq revealed *REST* as one of the genes upregulated upon depletion of MYCN. De-repression of REST was also confirmed at the protein level in both cell-lines using two different siRNAs (Figure 7A). Furthermore, we found that the REST-repressed target genes *STMN3*, *GDAP1* and *ENAH* were decreased after MYCN knockdown, consistent with the upregulation of functional REST protein (Figure 7B). To query the effect of MYCN on REST-regulated genes in WT, we performed GSEA on our MYCN depletion transcriptomic data using gene signatures established in stem cell-derived neurons

(58) and embryonic stem cells (ESC) (59) (Figure 7C). Both gene sets were significantly downregulated in both WT cell-lines upon MYCN knockdown, suggesting a MYCN - REST regulatory axis in WT.

REST was found to be significantly repressed in cluster 2 of the TARGET – WT data set (Figure 7D), which contained tumours with MYCN signature. In contrast, ESC-specific REST target genes were derepressed in the same group of tumours, as indicated by the expression of REST target metagene, representing overall expression of MYCN regulated REST genes of the signature described by Johnson et al. (59) (Figure 7E). We also found *REST* significantly repressed in WT as compared to fetal kidney in our cohort of primary samples (Figure 7F). Expression of *MYCN* and *REST* showed a strong, inverse correlation in these tissues ($R = -0.73$, $p = 0.0003$) (Figure 7G). Thus our data identifies the repression of the presumptive WT tumour suppressor gene *REST* as a hitherto uncharacterised oncogenic pathway downstream of MYCN deregulation.

Taken together, this study demonstrates that MYCN promotes growth and survival in WT via regulating multiple genes affecting splicing, translation, post-translational modification, microRNAs, metabolism and cellular differentiation (Figure 8). The intersection of MYCN with co-operative oncogenic and tumour suppressor pathways represent possible vulnerabilities of poor-prognosis Wilms' tumour which can be exploited in the future for urgently required targeted therapeutics.

Legends

Figure 1. Immunohistochemistry in fetal kidney and Wilms' tumours reveals a blastemal expression for MYCN protein in tumours.

MYCN expression was detected in the distal tubules (Dt) in 13-weeks-old fetal kidney, while the blastema (Bl), stroma (St) and proximal tubules (Pt) were negative. Blastemal-rich WT showed positivity in the blastemal component. Epithelial and stromal structures did not show any expression of MYCN protein. A table summarizing positive MYCN staining in the nucleus or the cytoplasm only in WT, according to histology, is shown underneath.

Figure 2. MYCN depletion leads to significant growth inhibition in anaplastic WT cell-lines.

(A) MYCN depletion resulted in significant growth suppression after 120 hours treatment in Wit49, but not in an increase in dead cells, using two different siRNAs. ($n = 3$, *** $p < 0.01$, two-tailed T-tests). **(B)** MYCN knockdown also led to significant growth suppression in 17.94 cells after 120 hours ($n = 3$). Western blot was used to confirm knockdown of MYCN in both cell-lines.

Figure 3. Genes and pathways identified by RNA-seq in MYCN-depleted anaplastic WT cells.

(A) Venn diagrams showing highly significant overlaps between differentially expressed genes (DEGs) in Wit49 and 17.94 after MYCN depletion for 48 hours, for up- and downregulated genes, respectively. DEGs were determined as statistically significant ($p < 0.05$) and having a minimum shrunk fold change, a conservative corrected value, of 1.2, calculated by using DESEQ2. The probability values for shared genes is indicated. **(B)** Heatmap of shared 561 DEGs in Wit49 and 17.94. Examples of known MYCN target genes are shown in black, while genes

associated with kidney development or Wilms' tumour predisposition are highlighted in green. **(C)** Validation of identified, select MYCN-regulated genes in WT cells by qPCR, 48 hours after MYCN knockdown. A representative of three biological replicates is shown. Significance was calculated based on the biological replicates (* $p < 0.05$, T-tests). **(D)** Venn diagram showing overlaps of MYCN-regulated genes in WT, described in this study, with MYCN target genes identified in neuroblastoma. **(E)** GSEA plots showing upregulation of gene signatures repressed in WT as compared to FK, upon depletion of MYCN. MYCN-activated genes of the MYCN157 signature, identified in NB, were downregulated. Examples of GSEA of downregulated GO gene sets associated with ribosomal and mitochondrial function and splicing in MYCN depleted WT cells. **(F)** Volcano plots of Gene Set Enrichment Analysis on MYCN depletion transcriptomes in WT cells. Normalized enrichment scores and False discovery rates (FDR) were calculated using Gene Ontology gene categories indicated universal downregulation of gene sets linked to ribosomal and mitochondrial function as well as those associated with RNA processing and splicing. Scores of all gene sets are shown in grey, while those of statistically significant gene sets (FDR < 0.05) in the highlighted, functional categories are indicated according to the legend.

Figure 4. Meta-analysis of MYCN regulated genes in the WT TARGET data set identifies distinct patient clusters.

(A) Overall expression of MYCN activated genes, identified as shared downregulated hits in MYCN depleted WT cells, showed a strong and significant positive correlation with MYCN expression in the TARGET-WT data set (SRP012006), containing transcriptomic data of 124 high-risk WT. Overall expression of MYCN repressed genes displayed a modest, inverse correlation that

did not reach significance. **(B)** K means clustering (K = 2) performed on TARGET-WT data set based on the expression of 561 MYCN regulated genes in WT, identified in this study. Clinical information is shown a as coloured bars on the top: stage (red = 1, green = 2, blue = 3, magenta = 3b, light green = 4, yellow = 5_3B, turquoise = 5_4); event type (none = red, blue = relapse, green = progression); vital status (green = alive, red = dead) and reason for death (green = none, yellow = tumour, red = infection, blue = toxicity, magenta = tumour and toxicity). **(C)** Proportion of tumours with various clinical stages. Chi-square test showed that the association of clinical stages with clustering according to MYCN-regulated genes is significant. Stages represented by a single tumour were omitted. **(D)** More death occurred in patients with tumours in cluster 2, however this association did not reach significance. **(E)** Overall expression of ribosome genes, mitochondrial protein complexes and methylosome components was significantly higher in cluster 2 tumours as compared to those in cluster 1 (ANOVA).

Figure 5. MYCN regulates *TOMM20* and other mitochondrial function genes. **(A)** GSEA showing downregulation of genes encoding for mitochondrial protein complexes with MYCN depletion. **(B)** Heatmap displaying the expression of the top 20 genes in the leading edge of the GO mitochondrial protein complex gene category in MYCN depleted in WT cells. **(C)** Validation of select mitochondrial genes in Wit49 and 17.94 cells by qPCR, 48 hours after MYCN knockdown. A representative of three biological replicates are shown. T-tests were performed on the biological replicates (* $p < 0.05$). **(D)** Western blot and quantification showing reduction of TOMM20 protein expression after 72 hours of MYCN depletion. (n = 3). **(E)** Expression of *MYCN* and *TOMM20* genes significantly correlated in the TARGET-WT data set (SRP012006). **(F)** Relapsed WT had significantly higher

549 expression of *TOMM20* mRNA than non-relapsed ones, as detected in GSE10320.
550 **(G)** *TOMM20* was also more highly expressed in blastemal WT than in tumours with
551 other histology (GSE31403).

552 **Figure 6. MYCN activates methylosome genes in WT.**
553 **(A)** Heatmap of genes encoding for methylosome components, showing expression
554 in MYCN-depleted WT cells. Genes highlighted in black were identified in this study
555 as significantly and substantially regulated by MYCN in two anaplastic WT cells. **(B)**
556 Validation of select methylosome genes in WT cells by qPCR, 48 hours after MYCN
557 knockdown. Statistical significance was calculated based on biological replicates
558 and expression for one representative is shown (* $p < 0.05$). **(C)** Western blot of
559 select methylosome components in WT cells 72 hours after MYCN knock-down with
560 two different siRNAs (n = 3). Protein expression was calculated based on
561 densitometry and normalized for the loading control on the same filter. Confirmation
562 of MYCN depletion is shown in Figure 5D. **(D)** *PRMT1* and **(E)** *WDR77*, encoding
563 for MEP50, were shown to be expressed at significantly higher levels in WT than in
564 fetal kidney (GSE6120).

565 **Figure 7. MYCN represses the WT predisposition gene *REST.***
566 **(A)** REST protein is derepressed upon MYCN depletion (n = 3). Protein expression
567 was calculated based on densitometry and normalized for loading control. **(B)**
568 Validation of upregulation of *REST* mRNA and downregulation of its target genes by
569 qPCR after MYCN depletion for 48 hours (n = 3). A representative experiment is
570 shown. T-tests were performed on biological replicates (* $p < 0.05$). **(C)** GSEA
571 showed downregulation of REST target genes with MYCN depletion. **(D)** REST has
572 a significantly lower expression in cluster 2 tumours in TARGET-WT data set
573 (SRP012006) as compared to cluster 1 (ANOVA). **(E)** REST target genes, showing

a significant overall overexpression in cluster 2 WT as compared to cluster 1. (ANOVA) **(F)** *REST* was found to be significantly repressed in WT as compared to FK by qPCR, as assessed by T-test. **(E)** Expression of *MYCN* and *REST* highly and significantly correlated in WT and FK, indicated by red and blue dots, respectively.

Figure 8. Model depicting select Wilms' tumour MYCN targets with potential functional consequences.

MYCN represses the *REST* tumour suppressor gene, which can result in activation of REST-repressed genes. *ROBO1* is also repressed, which may compromise the differentiation of the condensing mesenchyme (CM) into pre-tubular aggregates (PTA) via inhibition of SLIT-ROBO developmental signalling. The ureteric bud (UB) is also shown. MYCN activation of methylosome genes such as PRMTs alters arginine methylation (R-Me), with subsequent alterations in functions including mRNA splicing and protein stability. Activation of *TOMM20* by MYCN may lead to aberrant mitochondrial protein translocation (dashed red arrow) and altered tumour cell metabolism.

Supplementary figure 1. MYCN immunohistochemistry in adult human kidney.

MYCN protein is absent in fully differentiated and developed kidney.

Supplementary figure 2. Cell cycle analysis.

Depletion of MYCN protein in Wit49 cells by two different siRNAs for 72 hours resulted in a significant increase in the proportion of cells in G2/M phase and a decrease in S phase (n = 3, *** $p < 0.01$, T-test). No change was observed in the subG1 fraction. MYCN knock-down was confirmed by using Western blot. MYCN knock-down for Wit49 is also shown in Figure 7A.

Supplementary figure 3. Western blots of MYCN and LIN28B and GSEA of differentiation gene signatures in WT.

(A) Confirmation of MYCN depletion in samples used for RNA-seq. **(B)** Western blot showing downregulation of LIN28B protein after MYCN depletion for 72H in WT cells. Blots of confirmation of MYCN knock-down are shown in Figure 7A for Wit49 and Figure 5D for 17.94. **(C)** GSEA showed upregulation of kidney developmental gene sets in MYCN-depleted WT cells. **(D)** Single cell signatures of differentiated cell types in the fetal kidney were upregulated, while genes associated with proliferating cells were down in MYCN knock-down WT cells.

Supplementary figure 4. GSEA analysis in transcriptomes of MYCN-depleted WT cells.

(A) Genes overexpressed in WT vs. fetal kidney were mostly downregulated. **(B)** GSEA showed downregulation of MYC/MYCN gene sets. **(C)** GSEA highlighted downregulation of gene sets associated with RNA export from the nucleus and upregulation of unfolded protein response genes.

Supplementary table 1. Oligonucleotides

Supplementary table 2. Antibodies

Supplementary table 3. Shared MYCN-regulated genes in Wit49 and 17.94.

Supplementary table 4. Gene Ontology analysis of MYCN-regulated genes in Wilms' tumour.

Author Contributions: Marianna Szemes: Conceptualization, Methodology, Formal analysis, Investigation, Validation, Data curation, Writing: Original draft, review and editing, Visualization, Supervision. Zsombor Melegh: Formal analysis, Investigation, Validation. Jacob Bellamy, Ji Hyun Park, Biyao Chen: Investigation, Validation.

621 Alexander Greenhough: Visualization. Daniel Catchpoole: Resources. Karim Malik:
622 Conceptualization, Methodology, Formal analysis, Investigation, Resources, Funding
623 acquisition, Supervision, Project administration, Writing: Original draft, review and
624 editing, Visualization.

625 **Funding:** We would like to thank the Children's Cancer and Leukaemia Group
626 (CCLGA 2017 01; CCLGA 2019 16), the Biotechnology and Biological Sciences
627 Research Council (BB/P008232/1) and the Showering Fund for funding this study.

628 **Acknowledgments:** We wish to thank Prof. Herman Yeger (University of Toronto)
629 and Dr. Keith Brown (University of Bristol) for kindly sharing the WT cell-lines, Wit49
630 and 17.94, respectively. We also would like to thank Drs. Jane Coghill and Christy
631 Waterfall at the University of Bristol Genomics Facility for assitance with
632 transcriptomics and Dr. Andy Herman for help with flow cytometry. We greatly
633 indebted to Ms Aysen Yuksei and Dr Michael Krivanek for construction of the tissue
634 microarrays and reviewing pathology data.

635 **Conflicts of Interest:** The authors declare no conflict of interest. The funders had no
636 role in the design of the study; in the collection, analyses, or interpretation of data; in
637 the writing of the manuscript, or in the decision to publish the results".

638

References

1. Green, D.M. (1997) Wilms' tumour. *Eur J Cancer*, **33**, 409-418; discussion 419-420.
2. Cotton, C.A., Peterson, S., Norkool, P.A., Takashima, J., Grigoriev, Y., Green, D.M. and Breslow, N.E. (2009) Early and late mortality after diagnosis of wilms tumor. *Journal of clinical oncology : official journal of the American Society of Clinical Oncology*, **27**, 1304-1309.
3. Pelletier, J., Bruening, W., Li, F.P., Haber, D.A., Glaser, T. and Housman, D.E. (1991) WT1 mutations contribute to abnormal genital system development and hereditary Wilms' tumour. *Nature*, **353**, 431-434.
4. Pritchard-Jones, K., Fleming, S., Davidson, D., Bickmore, W., Porteous, D., Gosden, C., Bard, J., Buckler, A., Pelletier, J., Housman, D. *et al.* (1990) The candidate Wilms' tumour gene is involved in genitourinary development. *Nature*, **346**, 194-197.
5. Bardeesy, N., Falkoff, D., Petruzzi, M.J., Nowak, N., Zabel, B., Adam, M., Aguiar, M.C., Grundy, P., Shows, T. and Pelletier, J. (1994) Anaplastic Wilms' tumour, a subtype displaying poor prognosis, harbours p53 gene mutations. *Nature genetics*, **7**, 91-97.
6. Koesters, R., Ridder, R., Kopp-Schneider, A., Betts, D., Adams, V., Niggli, F., Briner, J. and von Knebel Doeberitz, M. (1999) Mutational activation of the beta-catenin proto-oncogene is a common event in the development of Wilms' tumors. *Cancer Res*, **59**, 3880-3882.
7. Torrezan, G.T., Ferreira, E.N., Nakahata, A.M., Barros, B.D., Castro, M.T., Correa, B.R., Krepischi, A.C., Olivieri, E.H., Cunha, I.W., Tabori, U. *et al.* (2014) Recurrent somatic mutation in DROSHA induces microRNA profile changes in Wilms tumour. *Nature communications*, **5**, 4039.
8. Rakheja, D., Chen, K.S., Liu, Y., Shukla, A.A., Schmid, V., Chang, T.C., Khokhar, S., Wickiser, J.E., Karandikar, N.J., Malter, J.S. *et al.* (2014) Somatic mutations in DROSHA and DICER1 impair microRNA biogenesis through distinct mechanisms in Wilms tumours. *Nat Commun*, **2**, 4802.
9. Wegert, J., Ishaque, N., Vardapour, R., Georg, C., Gu, Z., Bieg, M., Ziegler, B., Bausenwein, S., Nourkami, N., Ludwig, N. *et al.* (2015) Mutations in the SIX1/2 Pathway and the DROSHA/DGCR8 miRNA Microprocessor Complex Underlie High-Risk Blastemal Type Wilms Tumors. *Cancer cell*, **27**, 298-311.
10. Mahamdallie, S.S., Hanks, S., Karlin, K.L., Zachariou, A., Perdeaux, E.R., Ruark, E., Shaw, C.A., Renwick, A., Ramsay, E., Yost, S. *et al.* (2015) Mutations in the transcriptional repressor REST predispose to Wilms tumor. *Nature genetics*, **47**, 1471-1474.
11. Williams, R.D., Al-Saadi, R., Chagtai, T., Popov, S., Messahel, B., Sebire, N., Gessler, M., Wegert, J., Graf, N., Leuschner, I. *et al.* (2010) Subtype-specific FBXW7 mutation and MYCN copy number gain in Wilms' tumor. *Clinical cancer research : an official journal of the American Association for Cancer Research*, **16**, 2036-2045.
12. Williams, R.D., Al-Saadi, R., Natrajan, R., Mackay, A., Chagtai, T., Little, S., Hing, S.N., Fenwick, K., Ashworth, A., Grundy, P. *et al.* (2011) Molecular profiling reveals frequent gain of MYCN and anaplasia-specific loss of 4q and 14q in Wilms tumor. *Genes, chromosomes & cancer*, **50**, 982-995.

13. Shaw, A.P., Poirier, V., Tyler, S., Mott, M., Berry, J. and Maitland, N.J. (1988) Expression of the N-myc oncogene in Wilms' tumour and related tissues. *Oncogene*, **3**, 143-149.
14. Zirn, B., Hartmann, O., Samans, B., Krause, M., Wittmann, S., Mertens, F., Graf, N., Eilers, M. and Gessler, M. (2006) Expression profiling of Wilms tumors reveals new candidate genes for different clinical parameters. *International journal of cancer. Journal international du cancer*, **118**, 1954-1962.
15. Wittmann, S., Wunder, C., Zirn, B., Furtwangler, R., Wegert, J., Graf, N. and Gessler, M. (2008) New prognostic markers revealed by evaluation of genes correlated with clinical parameters in Wilms tumors. *Genes, chromosomes & cancer*, **47**, 386-395.
16. Bates, C.M., Kharzai, S., Erwin, T., Rossant, J. and Parada, L.F. (2000) Role of N-myc in the developing mouse kidney. *Developmental biology*, **222**, 317-325.
17. Huang, M. and Weiss, W.A. (2013) Neuroblastoma and MYCN. *Cold Spring Harbor perspectives in medicine*, **3**, a014415.
18. Alami, J., Williams, B.R. and Yeger, H. (2003) Derivation and characterization of a Wilms' tumour cell line, WiT 49. *Int J Cancer*, **107**, 365-374.
19. Brown, K.W., Charles, A., Dallosso, A., White, G., Charlet, J., Standen, G.R. and Malik, K. (2012) Characterization of 17.94, a novel anaplastic Wilms' tumor cell line. *Cancer Genet*, **205**, 319-326.
20. Williams, R.D., Chagtai, T., Alcaide-German, M., Apps, J., Wegert, J., Popov, S., Vujanic, G., van Tinteren, H., van den Heuvel-Eibrink, M.M., Kool, M. *et al.* (2015) Multiple mechanisms of MYCN dysregulation in Wilms tumour. *Oncotarget*, **6**, 7232-7243.
21. Beckers, A., Van Peer, G., Carter, D.R., Gartlgruber, M., Herrmann, C., Agarwal, S., Helsmoortel, H.H., Althoff, K., Molenaar, J.J., Cheung, B.B. *et al.* (2015) MYCN-driven regulatory mechanisms controlling LIN28B in neuroblastoma. *Cancer Lett*, **366**, 123-132.
22. Urbach, A., Yermalovich, A., Zhang, J., Spina, C.S., Zhu, H., Perez-Atayde, A.R., Shukrun, R., Charlton, J., Sebire, N., Mifsud, W. *et al.* (2014) Lin28 sustains early renal progenitors and induces Wilms tumor. *Genes Dev*, **28**, 971-982.
23. Yermalovich, A.V., Osborne, J.K., Sousa, P., Han, A., Kinney, M.A., Chen, M.J., Robinton, D.A., Montie, H., Pearson, D.S., Wilson, S.B. *et al.* (2019) Lin28 and let-7 regulate the timing of cessation of murine nephrogenesis. *Nature communications*, **10**, 168.
24. Tsialikas, J. and Romer-Seibert, J. (2015) LIN28: roles and regulation in development and beyond. *Development*, **142**, 2397-2404.
25. Blockus, H. and Chedotal, A. (2016) Slit-Robo signaling. *Development*, **143**, 3037-3044.
26. Xian, J., Aitchison, A., Bobrow, L., Corbett, G., Pannell, R., Rabbitts, T. and Rabbitts, P. (2004) Targeted disruption of the 3p12 gene, Dutt1/Robo1, predisposes mice to lung adenocarcinomas and lymphomas with methylation of the gene promoter. *Cancer Res*, **64**, 6432-6437.
27. Grieshammer, U., Le, M., Plump, A.S., Wang, F., Tessier-Lavigne, M. and Martin, G.R. (2004) SLIT2-mediated ROBO2 signaling restricts kidney induction to a single site. *Dev Cell*, **6**, 709-717.

28. Piper, M., Georgas, K., Yamada, T. and Little, M. (2000) Expression of the vertebrate Slit gene family and their putative receptors, the Robo genes, in the developing murine kidney. *Mech Dev*, **94**, 213-217.
29. Astuti, D., Da Silva, N.F., Dallol, A., Gentle, D., Martinsson, T., Kogner, P., Grundy, R., Kishida, T., Yao, M., Latif, F. *et al.* (2004) SLIT2 promoter methylation analysis in neuroblastoma, Wilms' tumour and renal cell carcinoma. *Br J Cancer*, **90**, 515-521.
30. Menon, R., Otto, E.A., Kokoruda, A., Zhou, J., Zhang, Z., Yoon, E., Chen, Y.C., Troyanskaya, O., Spence, J.R., Kretzler, M. *et al.* (2018) Single-cell analysis of progenitor cell dynamics and lineage specification in the human fetal kidney. *Development*, **145**.
31. Fan, R., Grignon, D., Gulcicek, E.E., Faught, P. and Cheng, L. (2011) Proteomic studies of Anaplasia in Wilms Tumor. *Proteomics Insights*, **4**.
32. Valentijn, L.J., Koster, J., Haneveld, F., Aissa, R.A., van Sluis, P., Broekmans, M.E., Molenaar, J.J., van Nes, J. and Versteeg, R. (2012) Functional MYCN signature predicts outcome of neuroblastoma irrespective of MYCN amplification. *Proc Natl Acad Sci U S A*, **109**, 19190-19195.
33. Boon, K., Caron, H.N., van Asperen, R., Valentijn, L., Hermus, M.C., van Sluis, P., Roobeek, I., Weis, I., Voute, P.A., Schwab, M. *et al.* (2001) N-myc enhances the expression of a large set of genes functioning in ribosome biogenesis and protein synthesis. *EMBO J*, **20**, 1383-1393.
34. Hsu, C.L., Chang, H.Y., Chang, J.Y., Hsu, W.M., Huang, H.C. and Juan, H.F. (2016) Unveiling MYCN regulatory networks in neuroblastoma via integrative analysis of heterogeneous genomics data. *Oncotarget*, **7**, 36293-36310.
35. Li, C.M., Kim, C.E., Margolin, A.A., Guo, M., Zhu, J., Mason, J.M., Hensle, T.W., Murty, V.V., Grundy, P.E., Fearon, E.R. *et al.* (2004) CTNNB1 mutations and overexpression of Wnt/beta-catenin target genes in WT1-mutant Wilms' tumors. *Am J Pathol*, **165**, 1943-1953.
36. Liberzon, A., Birger, C., Thorvaldsdottir, H., Ghandi, M., Mesirov, J.P. and Tamayo, P. (2015) The Molecular Signatures Database (MSigDB) hallmark gene set collection. *Cell Syst*, **1**, 417-425.
37. Montemurro, L., Raieli, S., Angelucci, S., Bartolucci, D., Amadesi, C., Lampis, S., Scardovi, A.L., Venturelli, L., Nieddu, G., Cerisoli, L. *et al.* (2019) A Novel MYCN-Specific Antigene Oligonucleotide Deregulates Mitochondria and Inhibits Tumor Growth in MYCN-Amplified Neuroblastoma. *Cancer Res*, **79**, 6166-6177.
38. Hald, O.H., Olsen, L., Gallo-Oller, G., Elfman, L.H.M., Lokke, C., Kogner, P., Sveinbjornsson, B., Flaegstad, T., Johnsen, J.I. and Einvik, C. (2019) Inhibitors of ribosome biogenesis repress the growth of MYCN-amplified neuroblastoma. *Oncogene*, **38**, 2800-2813.
39. Zhang, S., Wei, J.S., Li, S.Q., Badgett, T.C., Song, Y.K., Agarwal, S., Coarfa, C., Tolman, C., Hurd, L., Liao, H. *et al.* (2016) MYCN controls an alternative RNA splicing program in high-risk metastatic neuroblastoma. *Cancer Lett*, **371**, 214-224.
40. Oliynyk, G., Ruiz-Perez, M.V., Sainero-Alcolado, L., Dzieran, J., Zirath, H., Gallart-Ayala, H., Wheelock, C.E., Johansson, H.J., Nilsson, R., Lehtio, J. *et al.* (2019) MYCN-enhanced Oxidative and Glycolytic Metabolism Reveals Vulnerabilities for Targeting Neuroblastoma. *iScience*, **21**, 188-204.
41. Viswanathan, S.R., Powers, J.T., Einhorn, W., Hoshida, Y., Ng, T.L., Toffanin, S., O'Sullivan, M., Lu, J., Phillips, L.A., Lockhart, V.L. *et al.* (2009)

Lin28 promotes transformation and is associated with advanced human malignancies. *Nat Genet*, **41**, 843-848.

42. Pfanner, N. and Meijer, M. (1997) The Tom and Tim machine. *Curr Biol*, **7**, R100-103.
43. Dang, C.V., Le, A. and Gao, P. (2009) MYC-induced cancer cell energy metabolism and therapeutic opportunities. *Clin Cancer Res*, **15**, 6479-6483.
44. Huang, C.C., Gadd, S., Breslow, N., Cutcliffe, C., Sredni, S.T., Helenowski, I.B., Dome, J.S., Grundy, P.E., Green, D.M., Fritsch, M.K. *et al.* (2009) Predicting relapse in favorable histology Wilms tumor using gene expression analysis: a report from the Renal Tumor Committee of the Children's Oncology Group. *Clin Cancer Res*, **15**, 1770-1778.
45. Gadd, S., Huff, V., Huang, C.C., Ruteshouser, E.C., Dome, J.S., Grundy, P.E., Breslow, N., Jennings, L., Green, D.M., Beckwith, J.B. *et al.* (2012) Clinically relevant subsets identified by gene expression patterns support a revised ontogenic model of Wilms tumor: a Children's Oncology Group Study. *Neoplasia*, **14**, 742-756.
46. Park, S.H., Lee, A.R., Choi, K., Joung, S., Yoon, J.B. and Kim, S. (2019) TOMM20 as a potential therapeutic target of colorectal cancer. *BMB Rep*, **52**, 712-717.
47. Roche, M.E., Lin, Z., Whitaker-Menezes, D., Zhan, T., Szuhai, K., Bovee, J., Abraham, J.A., Jiang, W., Martinez-Outschoorn, U. and Basu-Mallick, A. (2020) Translocase of the outer mitochondrial membrane complex subunit 20 (TOMM20) facilitates cancer aggressiveness and therapeutic resistance in chondrosarcoma. *Biochim Biophys Acta Mol Basis Dis*, **1866**, 165962.
48. Feichtinger, R.G., Neureiter, D., Royer-Pokora, B., Mayr, J.A., Zimmermann, F.A., Jones, N., Koegler, C., Ratschek, M., Sperl, W. and Kofler, B. (2011) Heterogeneity of mitochondrial energy metabolism in classical triphasic Wilms' tumor. *Front Biosci (Elite Ed)*, **3**, 187-193.
49. Terada, K., Kanazawa, M., Yano, M., Hanson, B., Hoogenraad, N. and Mori, M. (1997) Participation of the import receptor Tom20 in protein import into mammalian mitochondria: analyses in vitro and in cultured cells. *FEBS Lett*, **403**, 309-312.
50. Westermann, F., Muth, D., Benner, A., Bauer, T., Henrich, K.O., Oberthuer, A., Brors, B., Beissbarth, T., Vandesompele, J., Pattyn, F. *et al.* (2008) Distinct transcriptional MYCN/c-MYC activities are associated with spontaneous regression or malignant progression in neuroblastomas. *Genome Biol*, **9**, R150.
51. Yang, Y. and Bedford, M.T. (2013) Protein arginine methyltransferases and cancer. *Nat Rev Cancer*, **13**, 37-50.
52. Park, J.H., Szemes, M., Vieira, G.C., Melegh, Z., Malik, S., Heesom, K.J., Von Wallwitz-Freitas, L., Greenhough, A., Brown, K.W., Zheng, Y.G. *et al.* (2015) Protein arginine methyltransferase 5 is a key regulator of the MYCN oncoprotein in neuroblastoma cells. *Mol Oncol*, **9**, 617-627.
53. Hua, Z.Y., Hansen, J.N., He, M., Dai, S.K., Choi, Y., Fulton, M.D., Lloyd, S.M., Szemes, M., Sen, J., Ding, H.F. *et al.* (2020) PRMT1 promotes neuroblastoma cell survival through ATF5. *Oncogenesis*, **9**, 50.
54. Chan-Penebre, E., Kuplast, K.G., Majer, C.R., Boriack-Sjodin, P.A., Wigle, T.J., Johnston, L.D., Rioux, N., Munchhof, M.J., Jin, L., Jacques, S.L. *et al.* (2015) A selective inhibitor of PRMT5 with in vivo and in vitro potency in MCL models. *Nat Chem Biol*, **11**, 432-437.

55. Fedoriw, A., Rajapurkar, S.R., O'Brien, S., Gerhart, S.V., Mitchell, L.H., Adams, N.D., Rioux, N., Lingaraj, T., Ribich, S.A., Pappalardi, M.B. *et al.* (2019) Anti-tumor Activity of the Type I PRMT Inhibitor, GSK3368715, Synergizes with PRMT5 Inhibition through MTAP Loss. *Cancer cell*, **36**, 100-114 e125.

56. Siu, L.L., Rasco, D.W., Vinay, S.P., Romano, P.M., Menis, J., Opdam, F.L., Heinhuis, K.M., Egger, J.L., Gorman, S.A., Parasrampuria, R. *et al.* (2019) METEOR-1: A phase I study of GSK3326595, a first-in-class protein arginine methyltransferase 5 (PRMT5) inhibitor, in advanced solid tumours. *Annals of Oncology*, **30**.

57. Ooi, L. and Wood, I.C. (2007) Chromatin crosstalk in development and disease: lessons from REST. *Nat Rev Genet*, **8**, 544-554.

58. Satoh, J., Kawana, N. and Yamamoto, Y. (2013) ChIP-Seq Data Mining: Remarkable Differences in NRSF/REST Target Genes between Human ESC and ESC-Derived Neurons. *Bioinform Biol Insights*, **7**, 357-368.

59. Johnson, R., Teh, C.H., Kunarso, G., Wong, K.Y., Srinivasan, G., Cooper, M.L., Volta, M., Chan, S.S., Lipovich, L., Pollard, S.M. *et al.* (2008) REST regulates distinct transcriptional networks in embryonic and neural stem cells. *PLoS Biol*, **6**, e256.

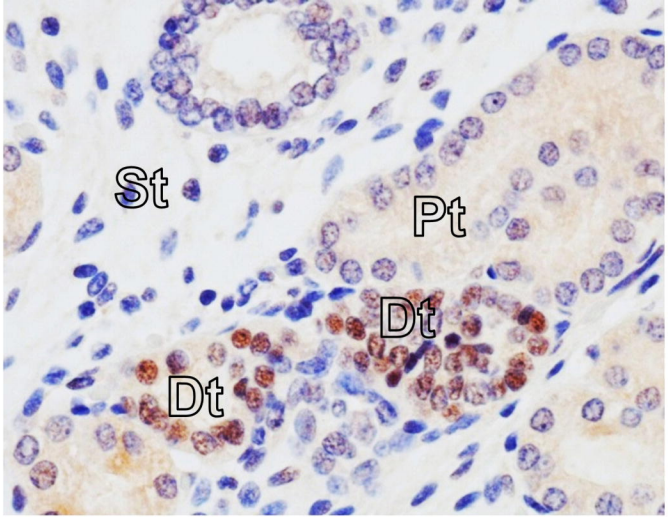

FK

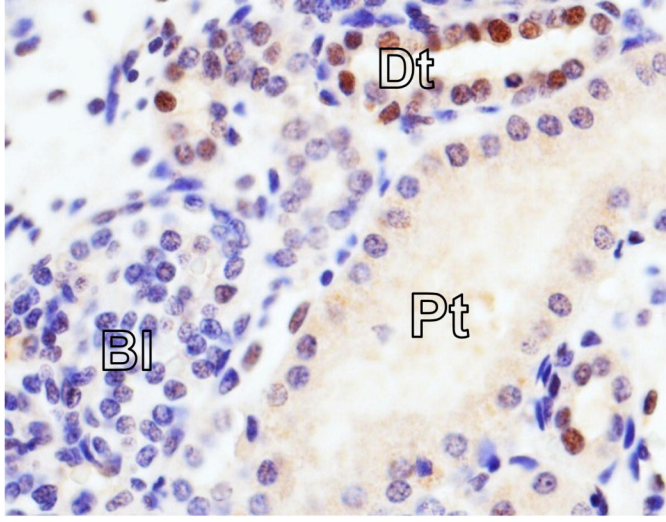

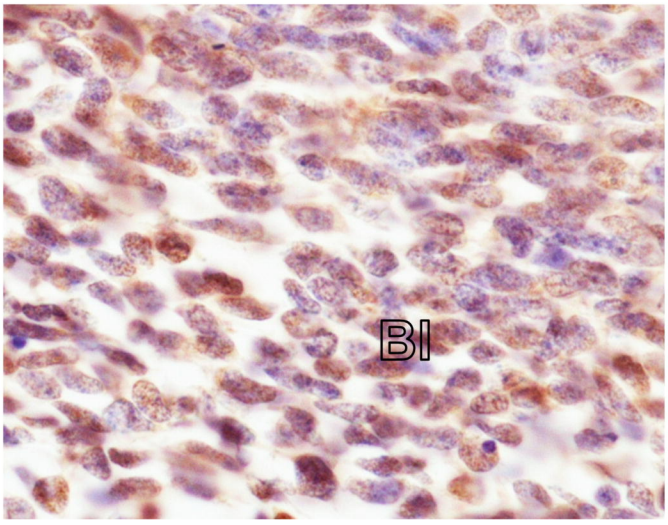

Blastemal-rich

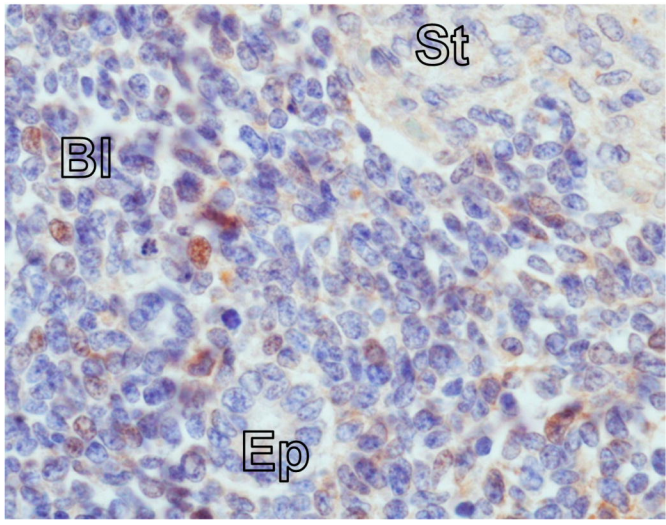

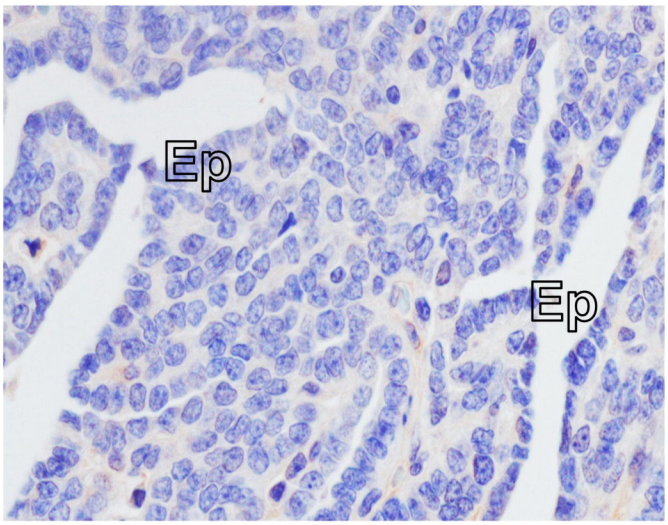

Epithelial/stromal

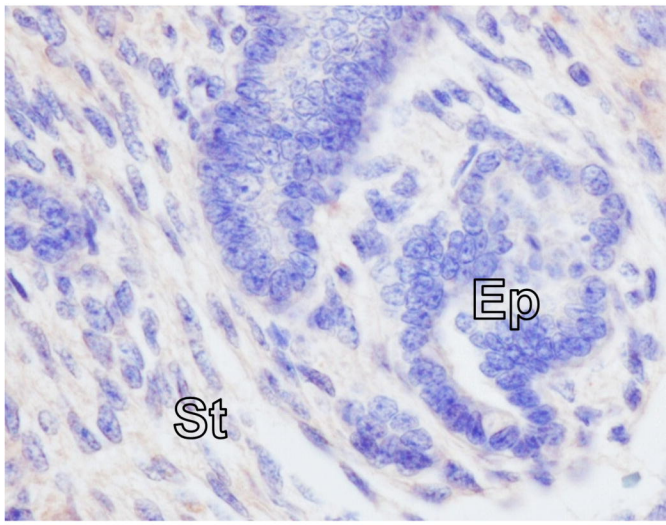

Pre-treatment	Nuclear +	Cyto only+	Neg	Total
Triphasic WT	7	3	12	22
Blastemal WT	2		3	5
Epithelial WT			1	1
Blastemal and	1			1
Blastemal and			1	1
Spindle cell	1			1
Not specified			2	2
Total	11	3	19	33

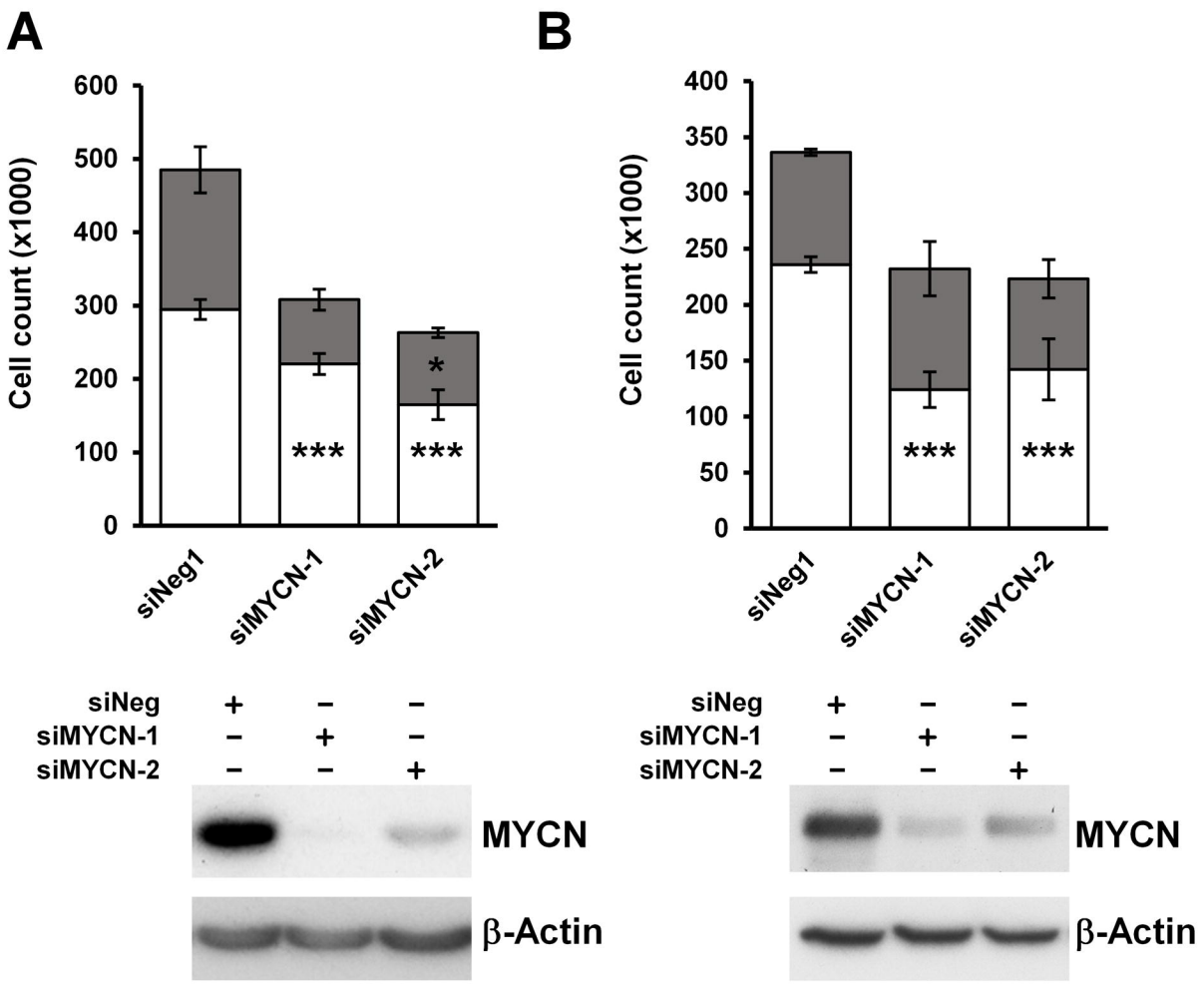
A
B
Cell count (x1000)
600
500
400
300
200
100
0
400
350
300
250
200
150
100
50
0
siNeg1
siMYCN-1
siMYCN-2
*
***
***
***
***
siNeg
siMYCN-1
siMYCN-2
+
−
−
−
+
−
−
−
+
MYCN
β-Actin

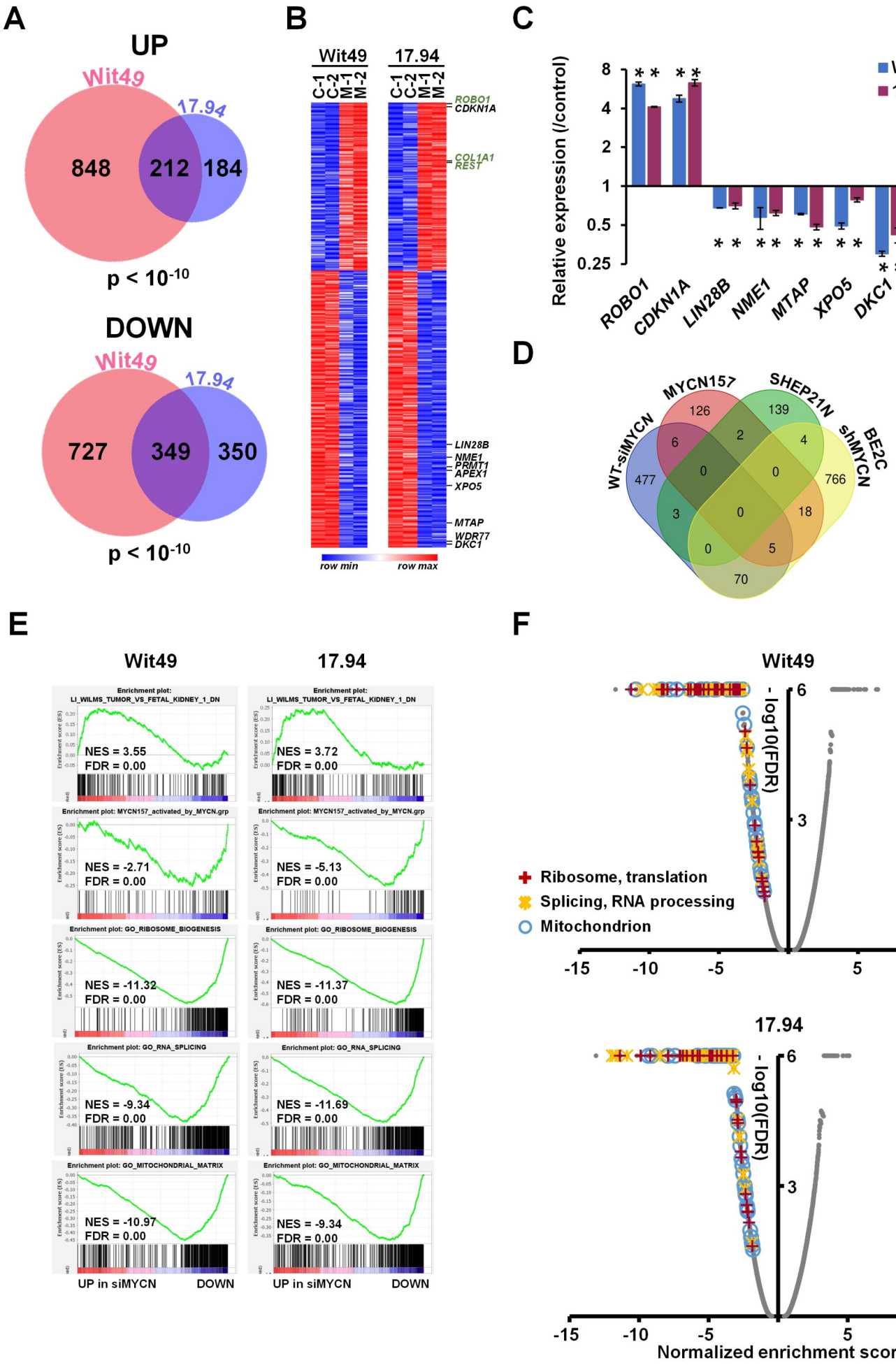
A
UP
Wit49
17.94
848
212
184
p < 10-10
DOWN
Wit49
17.94
727
349
350
p < 10-10
B
Wit49
17.94
C-1
C-2
M-1
M-2
ROBO1
CDKN1A
COL1A1
REST
LIN28B
NME1
PRMT1
APEX1
XPO5
MTAP
WDR77
DKC1
row min
row max
C
Relative expression (/control)
Wit49
17.94
ROBO1
CDKN1A
LIN28B
NME1
MTAP
XPO5
DKC1
D
MYCN157
SHEP21N
WT-siMYCN
BE2C shMYCN
126
139
6
2
4
477
0
0
766
3
0
18
0
5
70
E
Wit49
17.94
Enrichment plot: LI_WILMS_TUMOR_VS_FETAL_KIDNEY_1_DN
NES = 3.55
FDR = 0.00
NES = 3.72
FDR = 0.00
Enrichment plot: MYCN157_activated_by_MYCN.grp
NES = -2.71
FDR = 0.00
NES = -5.13
FDR = 0.00
Enrichment plot: GO_RIBOSOME_BIOGENESIS
NES = -11.32
FDR = 0.00
NES = -11.37
FDR = 0.00
Enrichment plot: GO_RNA_SPLICING
NES = -9.34
FDR = 0.00
NES = -11.69
FDR = 0.00
Enrichment plot: GO_MITOCHONDRIAL_MATRIX
NES = -10.97
FDR = 0.00
NES = -9.34
FDR = 0.00
UP in siMYCN
DOWN
UP in siMYCN
DOWN
F
Wit49
- log10(FDR)
Ribosome, translation
Splicing, RNA processing
Mitochondrion
17.94
- log10(FDR)
Normalized enrichment score

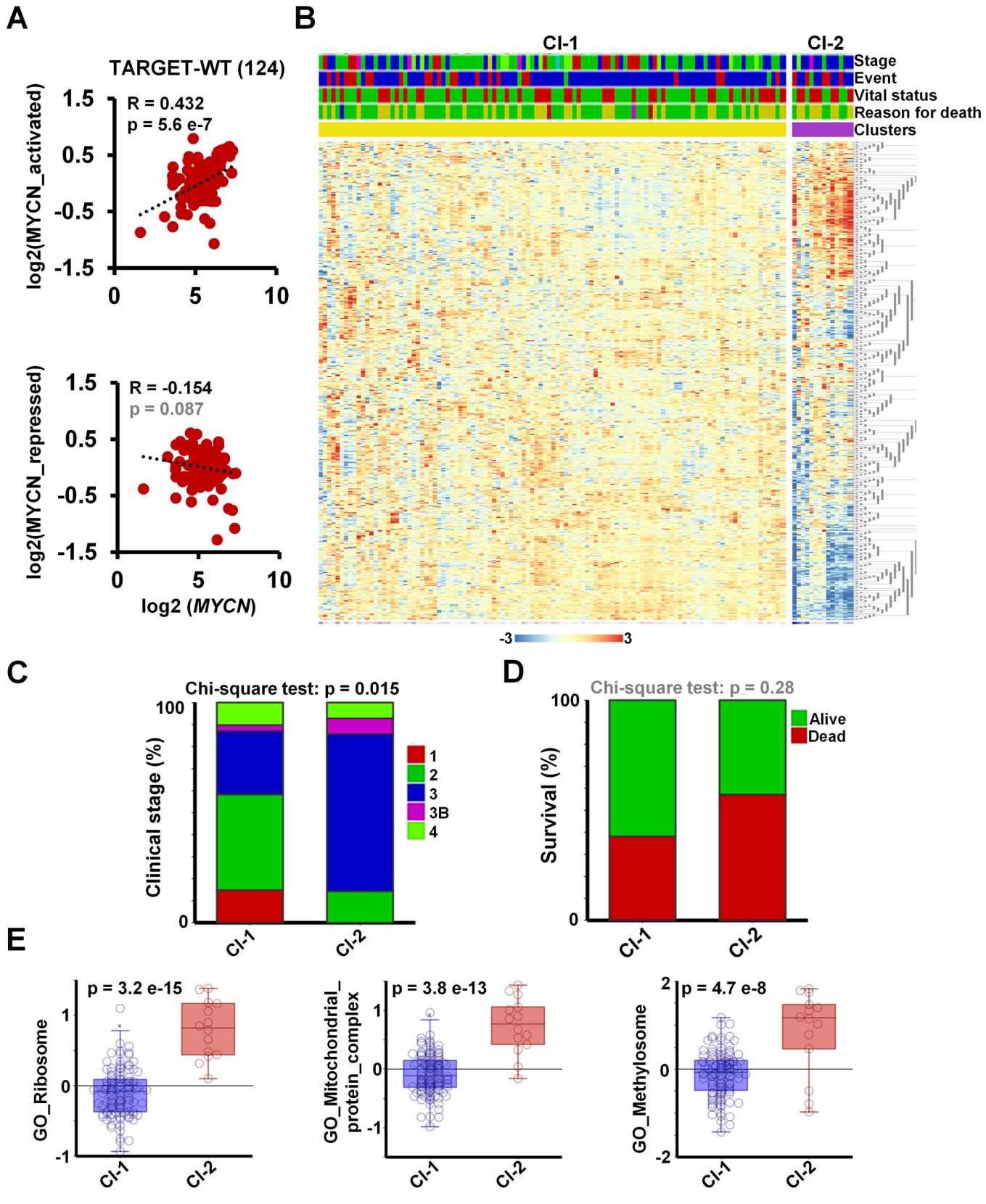
A
TARGET-WT (124)
R = 0.432
p = 5.6 e-7
log2(MYCN_activated)
R = -0.154
p = 0.087
log2(MYCN_repressed)
log2 (MYCN)
B
CI-1
CI-2
Stage
Event
Vital status
Reason for death
Clusters
-3
3
C
Chi-square test: p = 0.015
Clinical stage (%)
1
2
3
3B
4
D
Chi-square test: p = 0.28
Survival (%)
Alive
Dead
E
p = 3.2 e-15
GO_Ribosome
p = 3.8 e-13
GO_Mitochondrial_protein_complex
p = 4.7 e-8
GO_Methylosome

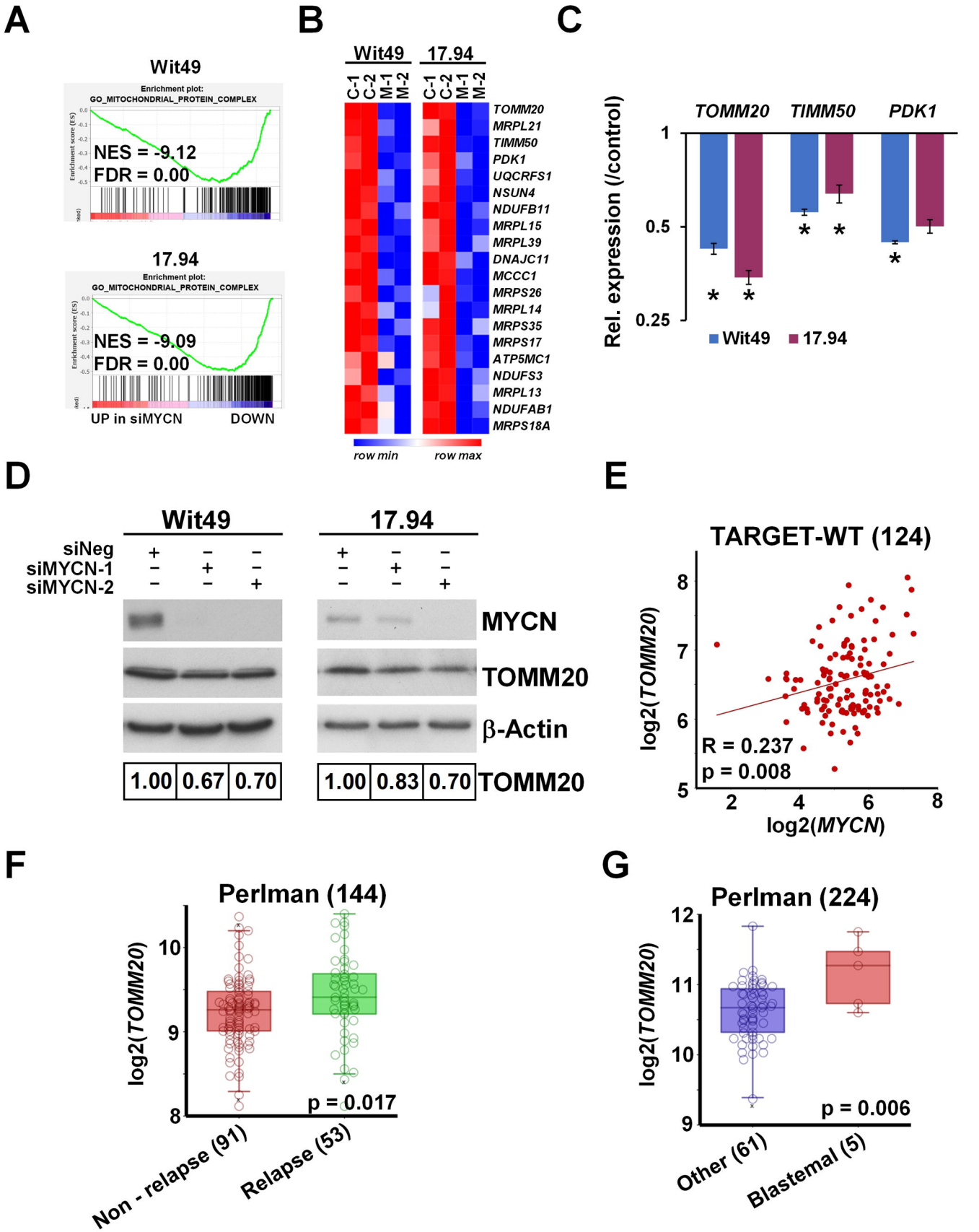
A
Wit49
Enrichment plot:
GO_MITOCHONDRIAL_PROTEIN_COMPLEX
NES = -9.12
FDR = 0.00
17.94
Enrichment plot:
GO_MITOCHONDRIAL_PROTEIN_COMPLEX
NES = -9.09
FDR = 0.00
UP in siMYCN
DOWN
B
Wit49
17.94
C-1
C-2
M-1
M-2
TOMM20
MRPL21
TIMM50
PDK1
UQCRFS1
NSUN4
NDUFB11
MRPL15
MRPL39
DNAJC11
MCCC1
MRPS26
MRPL14
MRPS35
MRPS17
ATP5MC1
NDUFS3
MRPL13
NDUFAB1
MRPS18A
row min
row max
C
TOMM20
TIMM50
PDK1
Rel. expression (/control)
1
0.5
0.25
Wit49
17.94
D
Wit49
17.94
siNeg
siMYCN-1
siMYCN-2
MYCN
TOMM20
β-Actin
1.00
0.67
0.70
1.00
0.83
0.70
TOMM20
E
TARGET-WT (124)
log2(TOMM20)
log2(MYCN)
R = 0.237
p = 0.008
F
Perlman (144)
log2(TOMM20)
p = 0.017
Non - relapse (91)
Relapse (53)
G
Perlman (224)
log2(TOMM20)
p = 0.006
Other (61)
Blastemal (5)

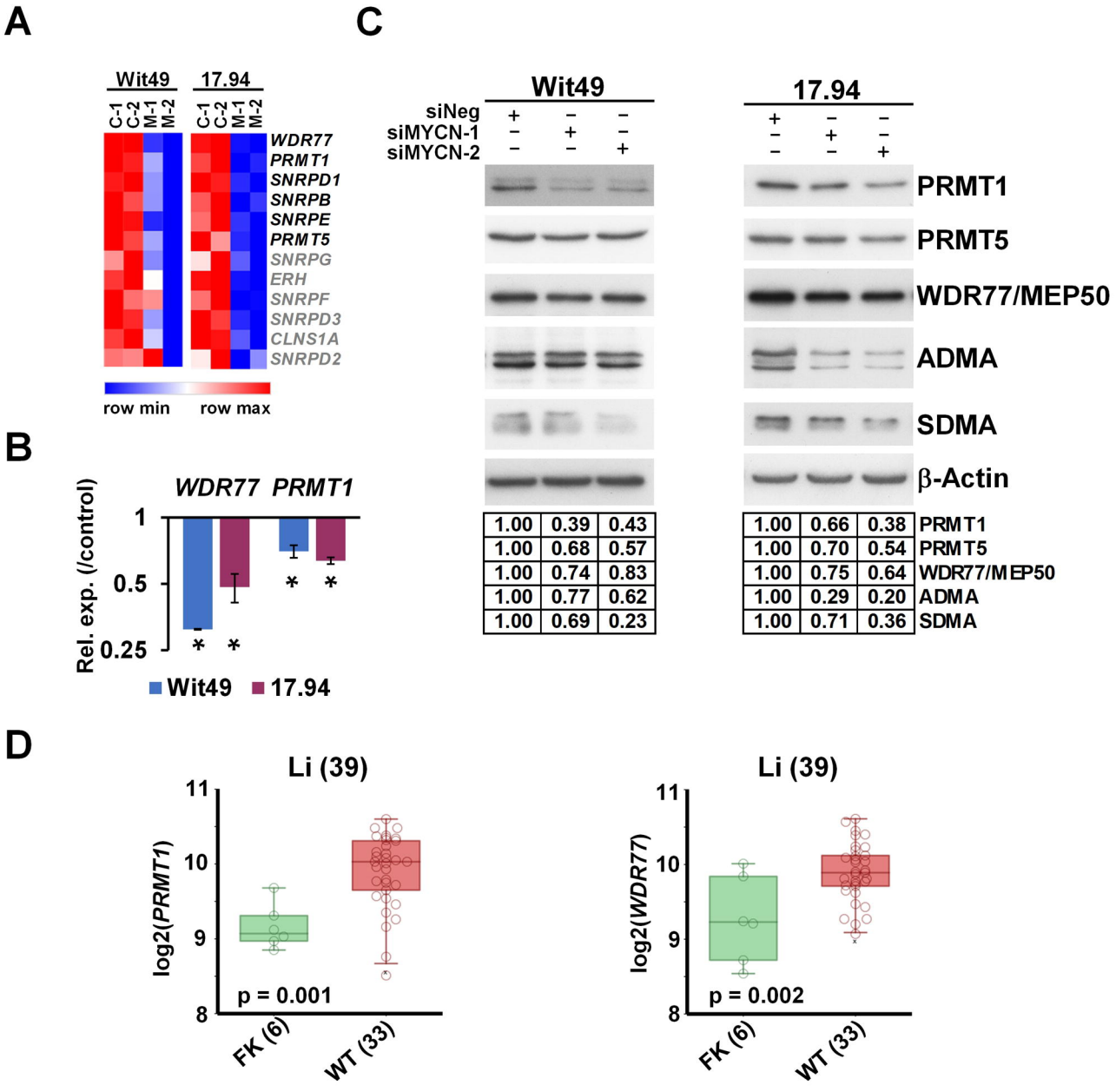
A
Wit49
17.94
C-1
C-2
M-1
M-2
WDR77
PRMT1
SNRPD1
SNRPB
SNRPE
PRMT5
SNRPG
ERH
SNRPF
SNRPD3
CLNS1A
SNRPD2
row min
row max
B
WDR77 PRMT1
Rel. exp. (/control)
1
0.5
0.25
Wit49
17.94
C
Wit49
17.94
siNeg
siMYCN-1
siMYCN-2
PRMT1
PRMT5
WDR77/MEP50
ADMA
SDMA
β-Actin
1.00 0.39 0.43 PRMT1
1.00 0.68 0.57 PRMT5
1.00 0.74 0.83 WDR77/MEP50
1.00 0.77 0.62 ADMA
1.00 0.69 0.23 SDMA
1.00 0.66 0.38 PRMT1
1.00 0.70 0.54 PRMT5
1.00 0.75 0.64 WDR77/MEP50
1.00 0.29 0.20 ADMA
1.00 0.71 0.36 SDMA
D
Li (39)
log2(PRMT1)
p = 0.001
FK (6)
WT (33)
Li (39)
log2(WDR77)
p = 0.002
FK (6)
WT (33)

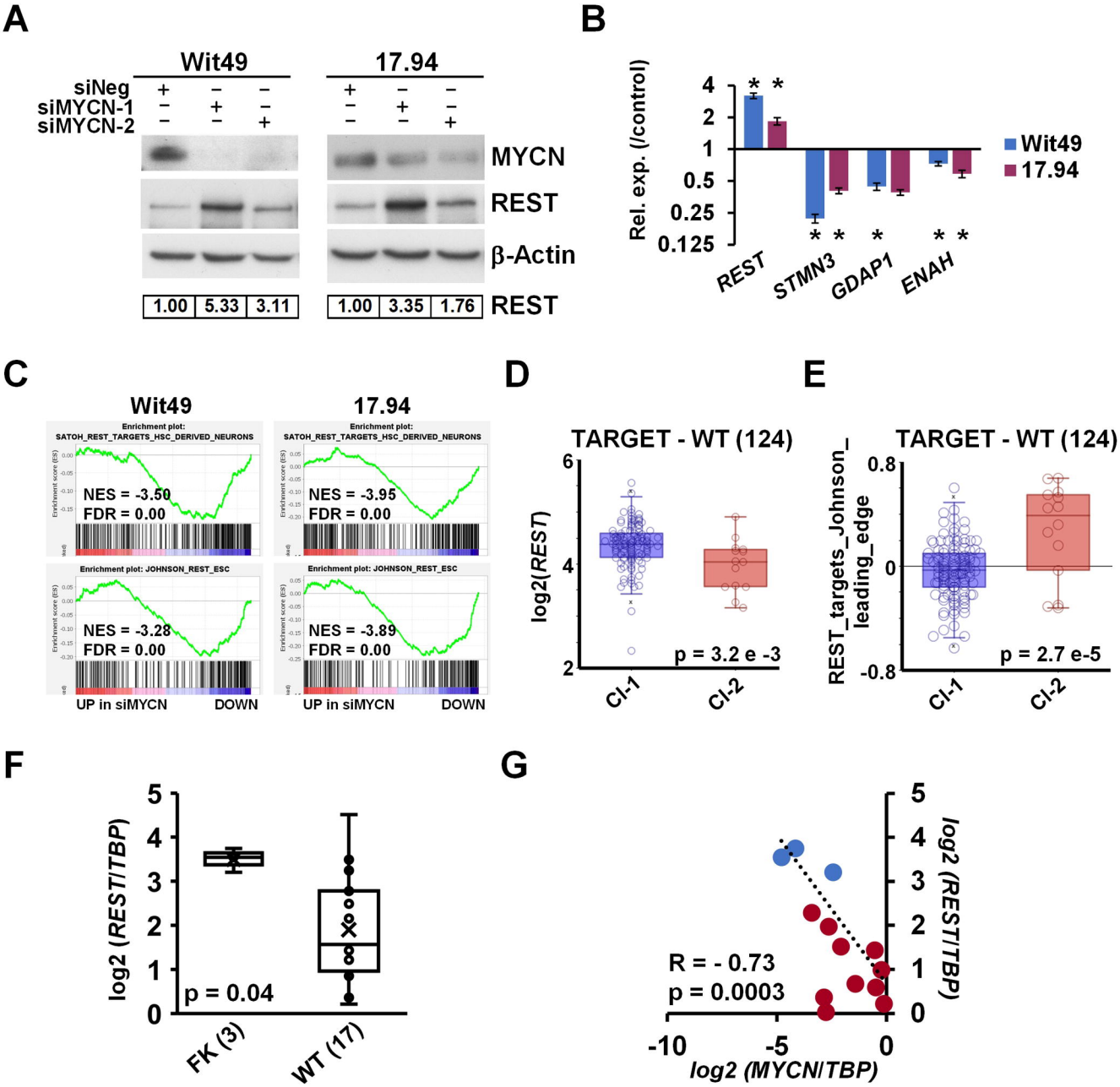
A
Wit49
17.94
siNeg
siMYCN-1
siMYCN-2
MYCN
REST
β-Actin
1.00 5.33 3.11
1.00 3.35 1.76
REST
B
Rel. exp. (/control)
4
2
1
0.5
0.25
0.125
REST
STMN3
GDAP1
ENAH
Wit49
17.94
C
Wit49
17.94
Enrichment plot: SATOH_REST_TARGETS_HSC_DERIVED_NEURONS
NES = -3.50
FDR = 0.00
NES = -3.95
FDR = 0.00
Enrichment plot: JOHNSON_REST_ESC
NES = -3.28
FDR = 0.00
NES = -3.89
FDR = 0.00
UP in siMYCN
DOWN
D
TARGET - WT (124)
log2(REST)
6
4
2
p = 3.2 e -3
CI-1
CI-2
E
TARGET - WT (124)
REST_targets_Johnson_leading_edge
0.8
0
-0.8
p = 2.7 e-5
CI-1
CI-2
F
log2 (REST/TBP)
5
4
3
2
1
0
p = 0.04
FK (3)
WT (17)
G
log2 (REST/TBP)
log2 (MYCN/TBP)
R = - 0.73
p = 0.0003
5
4
3
2
1
0
-10
-5
0

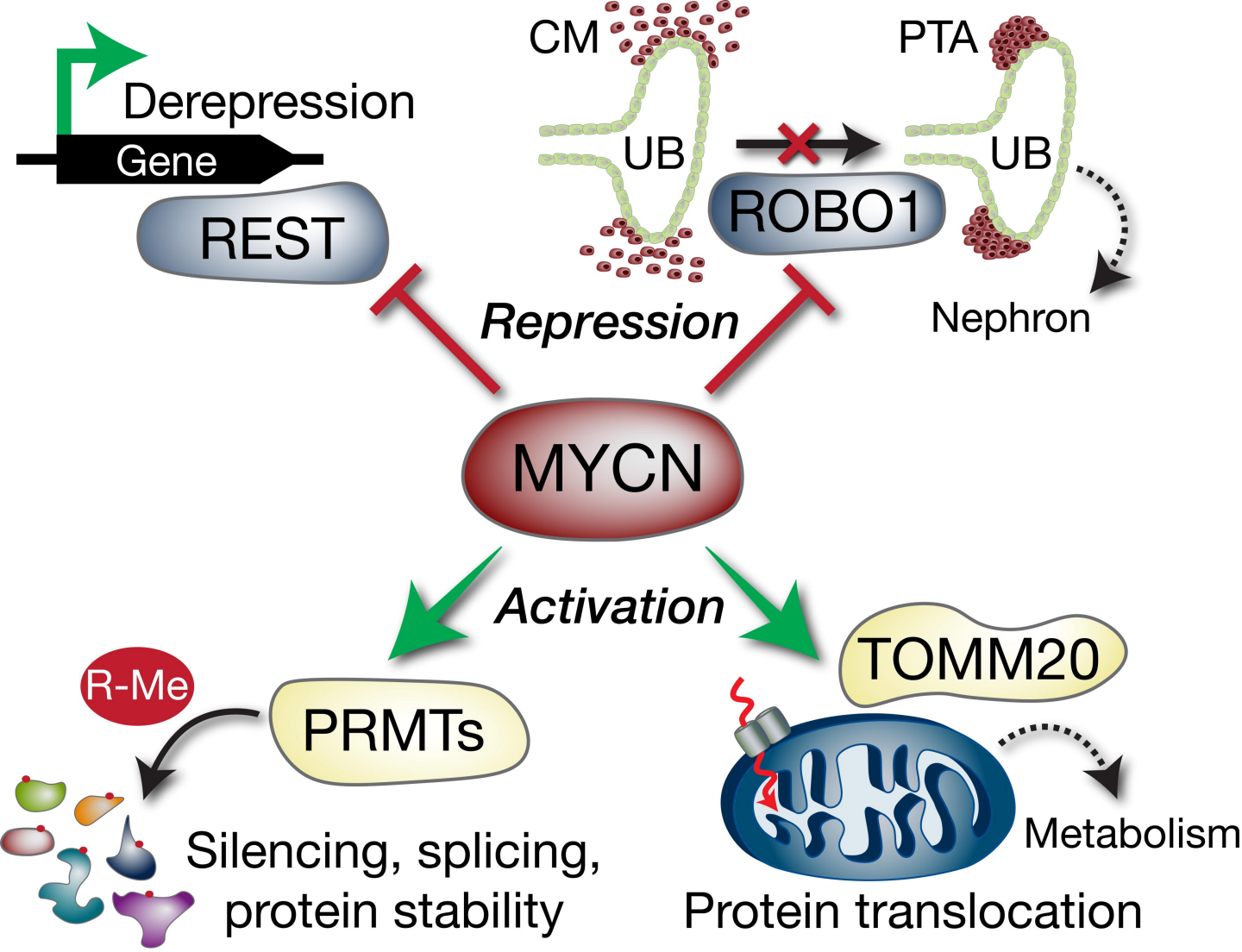
Derepression
Gene
REST
CM
UB
PTA
UB
ROBO1
Nephron
Repression
MYCN
Activation
R-Me
PRMTs
Silencing, splicing,
protein stability
TOMM20
Metabolism
Protein translocation